IMPORTANCE & APPLICATIONS OF NANOTECHNOLOGY

MEDDOCS
Open Access Publisher

Computer Simulation Study on Surface Composition of Bimetallic Nanocatalysts Synthesized in Microemulsion Template

Corresponding Author: Concha Tojo

Physical Chemistry Department, University of Vigo, E-36310, Vigo, Spain.

Email: ctojo@uvigo.es

Published Online: Nov 17, 2020

eBook: Importance & Applications of Nanotechnology

Publisher: MedDocs Publishers LLC

Online edition: http://meddocsonline.org/

Keywords: Nanocatalysts; Bimetallic nanoparticles; Microemulsion; One-pot method.

Abstract

A simulation study on the preparation of bimetallic nanocatalysts in microemulsion template was carried out to analyze the influence of different synthetic parameters on the composition of nanoparticle surface. In particular, the surface composition was studied by varying reduction rates of the two metals, reactants concentration and microemulsion composition. From this study, one can suggest that the enrichment in the slower metal at the surface is favored by microemulsions that provide of a rigid surfactant film. In addition, the enrichment is more pronounced as the reduction rate of the second metal is slower and as the reactants concentration is higher.

Bimetallic nanoparticles as catalysts

From the pioneering work of Sinfelt [1,2], the proposal of mix together two different metallic atoms to improve catalytic activity has been paid increasing attention [3-9]. Bimetallic catalysts have been proved to show a better catalytic behavior than usual monometallic ones [6,10-12], due to the so-called "electronic factor". It allows the movement of electrons from one metal to another because of partially filled d-band. For example, when Cu (filled d band) is added to Ni (incompletely filled d band), the extra electrons from Cu are included in the lattice, so electrons from Cu enter the Ni d band until it is filled. In this way, the degree of filling of the d band can be modified by varying the composition of the bimetallic catalyst [1]. As a result, the presence of a second metal modifies electronic interactions and heterometallic bonding interactions change the surface electronic properties of nanoparticles [8,10,12-17]. The overall efficiency observed in bimetallic catalysts accounts for synergistic effects [11,18-20]. This synergic/cooperative interaction is directly due to the electronic exchange between metals, which favors the reactants interaction, becomes more stable the reaction intermediates and facilitates the release of products. The result is an enhanced catalytic activity, reflected in the increasing progress in this field. A number of bimetallic catalysts are studied in different kinds of reactions, as shown in Table 1 (see also Table 1 in reference [21]).

Citation: Tojo C, (2020) Importance & Applications of Nanotechnology, MedDocs Publishers. Vol. 5, Chapter 1, pp. 1-7.

Table 1: Reactions catalyzed by bimetallic nanocatalysts.

Bimetallic nanocatalysts	Catalyzed reaction	References
Au-Ag	CO oxidation	[22]
Au-Pd	Suzuki and Heck reactions	[23]
Au-Pt	Oxygen reduction	[24]
Au-Pt	Oxygen reduction	[25]
Au-Pt	Methanol electrooxidation	[26]
Au-Pt	Oxygen reduction	[27]
Au-Pt	Methanol electrooxidation	[28]
Au-Pt	Coupling reactions	[19]
Cu-Fe	Coupling reactions	[29]
Pd-Ag	Formic acid oxidation	[30]
Pd-Ag	Glycerol oxidation	[31]
Pd-Ag	Ethanol oxidation	[32]
Pd-Sn	CO oxidation	[33]
Pt-Co	Oxygen reduction	[8]
Pt-Cu	Oxygen reduction	[34]
Pt-Pd	Hydrogenation	[35]
Pt-Pd	Electrosynthesis H_2O_2	[36]
Pt-Pd	Oxygen reduction	[37]
Pt-Ni	Hydrogenation	[38]
Pt-Ni	Oxygen reduction	[39]
Pt-Re	Reforming reactions	[40]
Pt-Sn	CO oxidation	[33]
Ni-Cu	Ethane hydrogenolysis	[1]
Ni-Cu	Cyclohexane dehydrogenation	[1]
Ni-Pd	Hydrogenation of nitrobenzene	[41]
Ro-Ir	Alkane hydrogenolysys	[42]
Ro-Fe	Alkane hydrogenolysys	[42]
Rh-Sn	Hydrogenation	[43]
Ru-Co	Oxidation of alcohols	[44]
Ru-Co	Diesel soot oxidation	[45]
Ru-Sn	Hydrogenation of polyenes	[46]
Ru-Ro	Hydrogenolysis of glycerol	[47]
Ni-Sn	CO oxidation	[33]

Futhermore, bimetallic nanocatalysts show additional advantages in relation to their stability when compared with monometallic ones. This is the case of Au-Pd nanocatalysts that catalyze the dehydrogenation reaction of formic acid. The presence of Au hinders the poisoning of the active sites of Pd by CO produced in a secondary reaction [11]. As a rule, the presence of the second metal can enhance the catalyst stability, which favors its recovery and recycling [21]. Finally, bimetallic nanocatalyst are arousing interest in green chemistry and future biomass-based refineries [47,48]. Comprehensive review articles on bimetallic nanocatalysts are already available [19,48-55].

The use of bimetallic nanocatalysts depends on the ability to design and tune the available active sites. A first factor to take into account is the nanocatalysts size. The catalyst are usually made up of small metal nanoparticles spread on an inert support. The catalytic activity of these particles depends on their size, since small ones show higher activity due to the greater number of atoms available on the particle surface. The second requirement is a precise control of the surface composition. A heterogeneous catalytic reaction occurs on the catalyst surface, on which the adsorption and desorption of reactants, intermediates and products take place. Therefore, the enhancement of catalysts performance is conditioned by the ability to control the arrangement of the two metallic atoms within the first atomic layers from the nanoparticle surface [28,54,56-58]. The optimal metal distribution at the surface depends on the particular reaction. For example, Au-Pt nanocatalysts were used to catalyze electro-oxidation of methanol, for which the best arrangement was a Pt-Au alloyed surface [26]. However, to catalyze oxygen reduction reaction and formic acid electrooxidation, a Pt shell on Au core arrangement showed a better catalytic activity. Because the ability to manipulate the surface composition of the bimetallic nanocatalysts is a key aspect to take into account, many efforts are being devoted to study innovative methods to synthesize bimetallic nanostructures with highly specific metal arrangements at the surface.

Bimetallic nanocatalysts from microemulsions

Among the available methods to produce nanoparticles, the water-in-oil microemulsion route is of great interest since this colloidal system favors the formation of catalysts in the nanosize range with narrow size distribution. The control of the particle size can be achieved by simply varying the water-to-surfactant molar ratio, which controls the size of the reversed micelles. Another advantage is that nanocatalyst are prepared at room temperature, while conventional methods of nanoparticle formation often require high temperatures, resulting in large nanoparticle sizes [59]. In addition, the special synthesis conditions provided by micelles lead frequently to catalytic material with improved catalytic properties [59]. Due to all these reasons, microemulsion route is one of the most favourite synthetic method to control the size and composition of bimetallic nanoparticles. The advances in this synthetic approach have been impressive in recent years and a number of different couples of bimetallic nanocatalysts have been propared from microemulsions (see reviews [59] and [60]].

Briefly, a microemulsion consists of water reverse micelles dispersed in the oil phase, and surrounded by a surfactant film. Reactants are dissolved in the water micelles, and can be exchanged between them by direct material transfer during an intermicellar collision [61]. By the intermicellar exchange, the reactants can be located in the same micelle, so chemical reaction can proceed inside the nanoreactor. The subsequent nucleation and growth of the particle are restricted because of the space limitation inside the micelle, giving rise to the formation of size-controlled particles.

Even though the reaction medium is complex, microemulsion route has several advantages when compared to traditional methods, as mentioned above. Nevertheless, research is needed for a better understanding of the microemulsion route due to the complication to managing the material intermicellar exchange. Initially, reactants are located in different micelles, so the whole process (reaction, nucleation and growth to build up final particles) depends on the material intermicellar exchange.

This exchange is dictated by the microemulsion composition, mainly by the surfactant, whose lipophilic portion is anchored into oil and the hydrophilic one into water. It gives rise to a film surrounding the micelle surface that can break up when a micelle-micelle collision is energetic enough, forming a transient dimer which allows the intermicellar exchange of material. This means that the exchange rate between micelles controls the reactants encounter, and, as a consequence, plays a key role in chemical kinetics in microemulsions, and has been shown to affect final nanoparticle properties [62-64].

Theoretical studies on the synthesis of nanoparticles in microemulsions are scarce and an enormous trial- and error- effort is needed to tune the bimetallic arrangement. A simulation model was developed with the aim of predicting the arrangement of final bimetallic nanoparticle. The validity of the model predictions was verified by comparing experimental and simulation results [65]. It is expected that theoretical researches will lead to a better understanding of this complex procedure and facilitate experimental trials. In the study at hand, we focus on the surface composition of the resulting nanoparticle predicted by simulation under different experimental conditions (changing microemulsion composition and reactants concentration) and for different couples of metals (changing the reduction rates). In this way, the model predictions can be used to establish practical guidelines to obtain bimetallic nanocatalysts.

Simulation model on the synthesis of bimetallic nanoparticles in microemulsions

The computer model simulates the kinetic course of the reaction (see reference [66] for details). Briefly, a set of micelles randomly positioned on a three dimensional square lattice represents the microemulsion. Reactants are initially distributed throughout micelles using a Poisson distribution. The one-pot method is recreated by mixing equal volumes of the microemulsions, each one containing one kind of reactant (reductor *R* and two metal salts A^+ and B^+).

An effective collision is simulated by chosing at random a 10% of micelles, which fuse and establish a channel between micelles, that permits the exchange of material. One Monte Carlo step finishes when the material carried by colliding micelles is modified obeying to the following criteria:

1. Reactants (A^+, B^+ and/or *R*) and free metal atoms (*A* and/or *B*) are transferred between colliding micelles according to the concentration gradient principle, i.e., material move from the more to the less concentrated micelle. The exchange parameter k_{ex} determines the maximum number of reactants and atoms that can be transferred.

2. The aggregation of metal atoms inside micelles gives rise to growing particles, whose exchange is limited by the channel size between colliding droplets, which depends on the flexibility of the surfactant film. The maximum particle size allowed to be transferred is quantified by the flexibility parameter (*f*). To include Ostwald ripening, when both colliding micelles are carrying particles, the smaller one moves to the micelle containing the greater one, if flexibility parameter allows the exchange.

The chemical reduction takes place when the metal salt (A^+ and/or B^+) and the reductor (*R*) are placed inside the same micelle after intermicellar redistribution of material during a collision. To simulate different reduction rates, a different percentage of the metal precursor carried by colliding micelles will be reduced, if there is enough reducing agent. In the case of Au salt (instantaneous reduction), 100% of Au salt is reduced. In order to test the influence of reduction rates, the second metal was characterized by a reduction rate of 50%, 20% and 10% of reactans inside colliding micelles can be reduced during a collision. For example, Au/Pt nanoparticles were successfully reproduced by simulation using a reduction rate 100% for Au, and 10% for Pt [65].

The surfactant film flexibility is included in the model by the k_{ex} (dimer stability) and the *f* (intermicellar channel size) parameters [67]. Thus, a flexible film, such as isooctane/tergitol/water, was successfully related to a channel size *f*=30, associated to k_{ex}=5 free atoms exchanged during a collision [65].

Each simulation run results in a set of micelles which can contain a particle, whose composition can be different. The sequence of metals deposition of each nanoparticle (which determines the metal segregation in final nanostructure) is monitored as a function on time. Then results are averaged over 1000 runs and the resulting sequence is divided in ten concentric layers (a spherical arrangement is assumed). Last of all the dispersion and averaged composition is calculated layer by layer.

Surface composition of bimetallic nanocatalysts synthesized in microemulsions

Previous studies showed that the main factors affecting to metal segregation are the difference between reduction rates of the two metals, concentration and microemulsion composition. It is expected that this influence will be reflected in the surface composition of final nanoparticle, so we will study each case as follows.

Influence of the metals reduction rates. Reduction potentials are directly related to the tendency of the salt to become reduced. It is assumed that the metal salt with a higher reduction potential metal will have the priority in reduction. If a one-pot method is used, both chemical reductions start at the same time. If in addition the reduction potentials are quite similar, the reductions take place at the same time, supporting the formation of an alloy due to the mix of the two metals from the beginning. As an example, Ag and Pd, whose reduction potentials are comparable ($\varepsilon^0 Ag^+/Ag$ = 0,80 V; $\varepsilon^0 Pd^{2+}/Pd$ = 0,915 V), were always obtained as alloys if prepared by a one-pot method in microemulsions [17,68,69]. Conversely, metals with different reduction potentials will give rise to segregated nanostructures, such as Au-Pt ($\varepsilon^0 AuCl_4^-/Au$ = 1,002 V; $\varepsilon^0 PtCl_6^{2-}/Pt$ = 0,742 V). The faster Au reduction gives rise to mostly Au core, surrounded by an enriched in Pt shell. Summarizing, the metal segregation is favored by a large difference between reduction potentials of the two metals composing the nanocatalysts.

Figure 1 shows simulations results on the distribution of particles with a given % of slower metal at the surface keeping constant the microemulsion composition (flexible film, *f*=30, k_{ex}=5) and the reactants concentration ($\langle c_{metal\ salts} \rangle$=16 reactants/micelle, $\langle c_R \rangle = 20 \langle c_{metal\ salts} \rangle$). Figures 1A, B, and C show results for different reduction rates of the slower reduction metal. 100% and 50% reduction rates shown in Figure 1A leads to a distribution in which most of the particles have an alloyed surface (72% particles have between 30 and 70% slow metal). As decreasing reduction rate of the slow metal (see Figures 1B & 1C), a progressive slow metal enrichment at surface is observed. In Figure 1B the slower reduction rate (20%) leads to a slightly enriched surface (72% particles have more than 60% slow metal at surface). When reduction rate is slower (see Figure 1C, 10%)

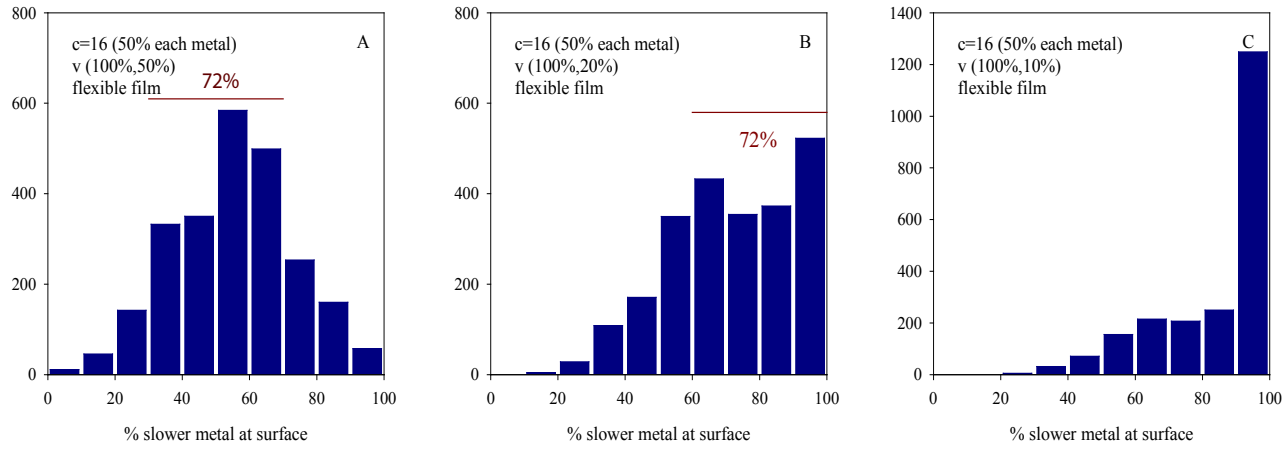

Figure 1: % of slower reduction metal at nanoparticle surface for different reduction rates and keeping fixed concentration ($\langle c_{metal\ salts} \rangle$=16 reactants/micelle, 50% of each reactant, ($\langle c_R \rangle$= 20 $\langle c_{metal\ salts} \rangle$) and microemulsion composition (flexible film, f=30, k_{ex}=5). In all cases, the faster reduction rate was 100% (all metal salts of the faster metal carried by colliding micelles are reduced at each effective collision). Figure 1A, B and C: A 50%, 20% and 10% of metal salts of the slower reduction metal are reduced at each effective collision, respectively.

the outer layer in most of particles is composed by 90-100% of slower metal. Therefore, the slower the reduction rate of the second metal, the higher the surface enrichment.

Influence of reactants concentration

Concentration of reactants inside micelles also affects metal segregation, since low concentrations favor the nanoalloy formation and high ones gives rise to more segregated structures [65]. To clearly observe the surface, Figure 2 shows particle distribution of the outer layer at different concentrations, keeping fixed reduction rates (100%, 20%) and microemulsion (f=30, k_{ex}=5, flexible film). The small concentration shown in Fig. 2A results mainly in an alloyed surface (73% of particles have between 30 and 70% slower metal at surface). As increasing concentration, the enrichment at the surface is more pronounced (see Figure 2B & 2C).

The transition from an alloyed to an enriched shell as concentration increases is also observed when the difference between reductions rates is larger. Figure 3 shows the surface distributions when the slower metal is ten times slower than the faster one. As one can see, enriched surfaces appear even at low concentrations (Figure 3A, 81% particles have more than 50% slower metal at surface). Higher concentrations result in more enriched surfaces. Thus, 57% particles show a pure surface at middle concentration (Figure 3B, c=16 reactants/micelle), while this percentage reaches 73% at high concentration (Figure 3C, c=32).

Influence of microemulsion composition

Some metals couples have been obtained as core-shell or alloyed arrangements using different microemulsions [70]. As a rule, rigid surfactant films result in the formation of better-segregated arrangements, while ones that are more flexible favor the alloy formation. It can be observed in Figure 4, that shows surface composition for different microemulsions and keeping fixed concentration and reduction rates. A progressive tendency to alloyed surfaces is observed as the film flexibility increases. So 73% of particles have an enriched shell (composed by more than 70% slow metal) when the film is rigid, and this percentage decreases to 53% for flexible films, and to only 24% if the film is very flexible. Therefore, the more flexible the film, the more alloyed surface.

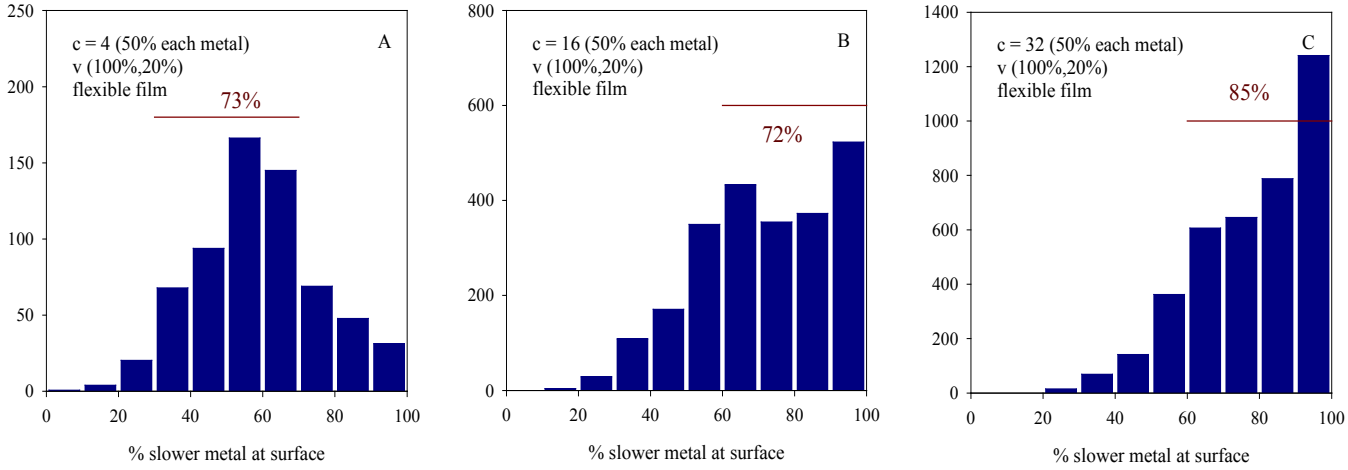

Figure 2: % of slower reduction metal at nanoparticle surface obtained at different values of concentration. Figures A, B and C show results at $\langle c_{metal\ salts} \rangle$ = 4, 16 and 32 reactants per micelles respectively (50% of each reactant, $\langle c_R \rangle$ = 20 $\langle c_{metal\ salts} \rangle$). The microemulsion composition (flexible film, f=30, k_{ex}=5) and the reduction rates (100% and 20%) were kept fixed.

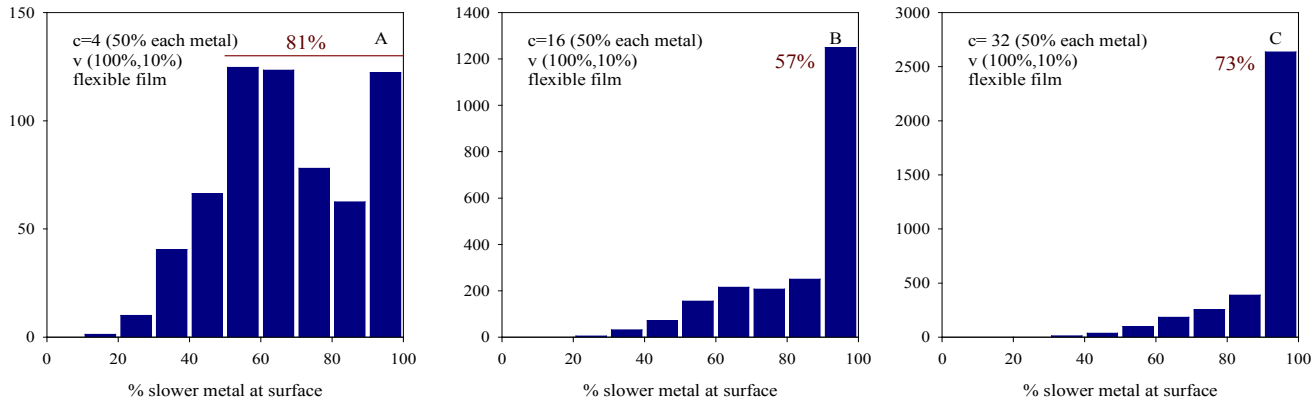

Figure 3: % of slower reduction metal at nanoparticle surface obtained at different values of concentration. Figures A, B and C show results at $\langle c_{metal\ salts} \rangle$ = 4, 16 and 32 reactants per micelles respectively (50% of each reactant, $\langle c_R \rangle = 20 \langle c_{metal\ salts} \rangle$). The microemulsion composition (flexible film, f=30, k_{ex}=5) and the reduction rates (100% and 10%) were kept fixed.

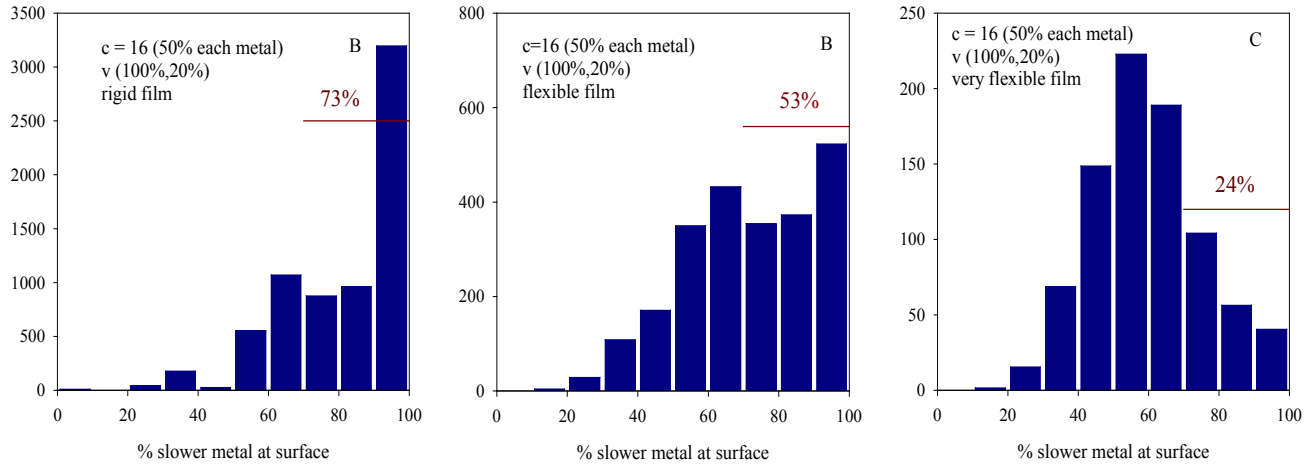

Figure 4: % of slower reduction metal at nanoparticle surface obtained at different values of the film flexibility. Figures A, B and C show results for a rigid (f=5, k_{ex}=1), flexible (f=30, k_{ex}=5) and very flexible (f=90, k_{ex}=15) surfactant film. Simulation parameters: $\langle c_{metal\ salts} \rangle$ = 16 reactants per micelle (50% of each reactant), $\langle c_R \rangle = 20 \langle c_{metal\ salts} \rangle$. Reduction rates are 100% and 20%.

Conclusions

The following guidelines to get a more enriched in the slower metal nanocatalysts surface can be proposed from simulation results: 1- As the reduction rate of the second metal is slower, the surface enrichment is higher. 2- As the concentration increases, the surface enrichment also increases. 3- As the film flexibility is more rigid, the surface enrichment is more pronounced.

References

1. Sinfelt JH. Catalysis by alloys and bimetallic clusters. Acc Chem Res. 1977; 10: 15-20.

2. Sinfelt JH. Structure of bimetallic clusters. Acc Chem Res. 1987; 20: 134-139.

3. Rojas S, García-García FJ, Jaeras S, Martínez-Huerta MV, García Fierro JL, et al. Preparation of carbon supported Pt and PtRu nanoparticles from microemulsion. Appl Catal, A. 2005; 285: 24-35.

4. Touroude R, Girard P, Maire G, Kizling J, Boutonnet M, et al. Preparation of colloidal platinum/palladium alloy particles from non-ionic microemulsions: Characterization and catalytic behaviour. Colloid Surface A. 1992; 67: 9-19.

5. Szumełda T, Drelinkiewicz A, Lalik E, Kosydar R, Duraczyńska D, et al. Carbon-supported Pd100-XAuX alloy nanoparticles for the electrocatalytic oxidation of formic acid: Influence of metal particles composition on activity enhancement. Applied Catalysis B: Environmental. 2018; 221: 393-405.

6. Vysakh AB, Babu CL, Vinod CP. Demonstration of synergistic catalysis in Au@ Ni bimetallic core-shell nanostructures. J Phys Chem C. 2015; 119: 8138-8146.

7. Heshmatpour F, Abazari R. Formation of dispersed palladium-nickel bimetallic nanoparticles in microemulsions: Synthesis, characterization, and their use as efficient heterogeneous recyclable catalysts for the amination reactions of aryl chlorides under mild conditions. RSC Adv. 2014; 4: 55815-55826.

8. Spanos I, Dideriksen K, Kirkensgaard JJK, Jelavic S, Arenz M. Structural disordering of de-alloyed Pt bimetallic nanocatalysts: The effect on oxygen reduction reaction activity and stability. Phys Chem Chem Phys. 2015; 17: 28044-28053.

9. Chaudhuri RG, Paria S. Core/Shell Nanoparticles: Classes, Properties, Synthesis Mechanisms, Characterization, and Applications. Chem Rev. 2012; 112: 2373-27433.

10. Bandarenka AS, Varela AS, Karamad M, Calle-Vallejo F, Bech L, et al. Design of an active site towards optimal electrocatalysis:

Overlayers, surface alloys and near-surface alloys of Cu/Pt (111). Angew Chem, Int Ed. 2012; 51: 11845-11848.

11. Gu X, Lu ZH, Jiang HL, Akita T, Xu Q. Synergistic catalysis of metal-organic framework-immobilized Au-Pd nanoparticles in dehydrogenation of formic acid for chemical hydrogen storage. J Am Chem Soc. 2011; 133: 11822-11825.

12. Zielinska-Jurek A, Kowalska E, Sobczak JW, Lisowski W, Ohtani B, et al. Preparation and characterization of monometallic (Au) and bimetallic (Ag/Au) modified-titania photocatalysts activated by visible light. Appl Catal, B. 2011; 101: 504-514.

13. Tedsree K, Li T, Jones S, Chan CWA, Yu KMK, et al. Hydrogen production from formic acid decomposition at room temperature using a Ag-Pd core-shell nanocatalyst. Nat Nanotechnol. 2011; 6: 302-307.

14. König RYG, Schwarze M, Schomäcker R, Stubenrauch C. Catalytic activity of mono- and bi-metallic nanoparticles synthesized via microemulsions. Catalysts. 2014; 4: 256-275.

15. Singh HP, Gupta N, Sharma SK, Sharma RK. Synthesis of bimetallic Pt-Cu nanoparticles and their application in the reduction of rhodamine B. Colloid Surface A. 2013; 416: 43-50.

16. Santhanalakshmi J, Venkatesan P. Mono and bimetallic nanoparticles of gold, silver and palladium-catalyzed NADH oxidation-coupled reduction of Eosin-Y. J Nanoparticle Res. 2011; 13: 479-490.

17. Heshmatpour F, Abazari R, Balalaie S. Preparation of monometallic (Pd, Ag) and bimetallic (Pd/Ag, Pd/Ni, Pd/Cu) nanoparticles via reversed micelles and their use in the Heck reaction. Tetrahedron. 2012; 68: 3001-3011.

18. Shi J. On the synergetic catalytic effect in heterogeneous nanocomposite catalysts. Chem Rev. 2013; 113: 2139-21 81.

19. Notar Francesco I, Fontaine-Vive F, Antoniotti S. Synergy in the catalytic activity of bimetallic nanoparticles and new synthetic methods for the preparation of fine chemicals. Chem Cat Chem. 2014; 6: 2784-2791.

20. Wen M, Mori K, Kuwahara Y, Yamashita H. Plasmonic Au@Pd nanoparticles supported on a basic metal-organic framework: Synergic boosting of H2 production from formic acid. ACS Energy Lett. 2017; 2: 1-7.

21. Rai RK, Tyagi D, Gupta K, Singh SK. Activated nanostructured bimetallic catalysts for C-C coupling reactions: Recent progress. Catal Sci Technol. 2016; 6: 3341-3361.

22. Wang AQ, Chang CM, Mou CY. Evolution of catalytic activity of Au-Ag bimetallic nanoparticles on mesoporous support for CO oxidation. J Phys Chem B. 2005; 109: 18860-18867.

23. Song HM, Moosa BA, Khashab NM. Water-dispersable hybrid Au–Pd nanoparticles as catalysts in ethanoloxidation, aqueous phase Suzuki–Miyaura and Heck reactions. J Mater Chem. 2012; 22: 15953 -15959.

24. Hernández-Fernández P, Rojas S, Ocón P, Gómez de la Fuente JL, San Fabián J, et al. Influence of the preparation route of bimetallic Pt-Au nanoparticle electrocatalyst for the oxygen reduction reaction. J Phys Chem B. 2007; 111: 2913-2923.

25. Félix-Navarro RM, Beltran-Gastelum M, Reynoso-Soto EA, Paraguay-Delgado F, Alonso-Núnez G, et al. Bimetallic Pt-Au nanoparticles supported on multi-wall carbon nanotubes as electrocatalysts for oxygen reduction. Renewable Energy. 2016; 87: 31-41.

26. Zhao L, Thomas JP, Heinig NF, Abd-Ellah M, Wang X, et al. Au-Pt alloy nanocatalysts for electro-oxidation of methanol and their application for fast-response non-enzymatic alcohol sensing. J Mater Chem C. 2014; 2: 2707-2714.

27. Shao M, Peles A, Shoemaker K, Gummalla M, Njoki PN, et al. Enhanced oxygen reduction activity of platinum monolayer on gold nanoparticles. J Phys Chem Lett 2011; 2: 67-72.

28. Suntivich J, Xu Z, Carlton CE, Kim J, Han B, et al. Surface composition tuning of Au-Pt bimetallic nanoparticles for enhanced carbon monoxide and methanol electro-oxidation. J Am Chem Soc. 2013; 135: 7985-7991.

29. Hudson R, Li C-J, Moores A. Magnetic copper-iron nanoparticles as simple heterogeneous catalysts for the azide-alkyne click reaction in water. Green Chem. 2012; 14: 622-624.

30. Liu D, Xie ML, Wang CM, Liao LW, Qiu L, et al. Pd-Ag alloy hollow nanostructures with interatomic charge polarization for enhanced electrocatalytic formic acid oxidation. Nano Res. 2016; 9: 1590-1599.

31. Hirasawa S, Watanabe H, Kizuka T, Nakagawa Y, Tomishige K, et al. Performance, structure and mechanism of Pd-Agalloy catalyst for selective oxidation of glycerol to dihydroxyacetone. J Catal. 2013; 300: 205-216.

32. Oliveira MC, Rego R, Fernandes LS, Tavares PB. Evaluation of the catalytic activity of Pd-Ag alloys on ethanoloxidation and oxygen reduction reactions in alkaline medium. J Power Sources. 2011; 196: 6092-6098.

33. Araña J, Ramírez de la Piscina P, Llorca J, Sales J, Homs N, et al. Bimetallic silica-supported catalysts based on Ni-Sn, Pd-Sn, and Pt-Sn as materials in the CO oxidation reaction. Chem Mater. 1998; 10: 1333-1342.

34. Koh S, Strasser P. Electrocatalysis on bimetallic surfaces: Modifying catalytic reactivity for oxygen reduction by voltammetric surface dealloying. J Am Chem Soc. 2007; 129: 12624-12625.

35. Navarro RM, Pawelec B, Trejo JM, Mariscal R, Fierro JLG. Hydrogenation of aromatics on sulfur-resistant PtPd bimetallic catalysts. J Catal. 2000; 189: 184-194.

36. Félix-Navarro RM, Beltran-Gastelum M, Salazar-Gastelum MI, Silva-Carrillo C, Reynoso-Soto EA, et al. Pt-Pd bimetallic nanoparticles on MWCNTs: Catalyst for hydrogen peroxide electrosynthesis. J Nanopart Res. 2013; 15: 1802/1-11.

37. Wang W, Vara M, Luo M, Huang H, Ruditskiy A, et al. Pd@Pt core–shell concave decahedra: A class of catalysts for the oxygen reduction reaction with enhanced activity and durability. J Am Chem Soc. 2015; 137: 15036-15042.

38. Cheney BA, Lauterbach JA, Chen JG. Reverse micelle synthesis and characterization of supported Pt/Ni bimetallic catalysts on γ-Al2O3. App Catal, A. 2011; 394: 41-47.

39. Gan L, Heggen M, Rudi S, Strasser P. Core-shell compositional fine structures of dealloyed PtxNi1-x nanoparticles and their impact on oxygen reduction catalysis. Nano Lett. 2012; 12: 5423-5430.

40. Parera JM, Beltramini JN. Stability of bimetallic reforming catalysts. J Catal. 1988; 112: 357-365.

41. Lu P, Teranishi T, Asakura K, Miyake M, Toshima N. Polymer-protected Ni/Pd bimetallic nano-clusters: Preparation, characterization and catalysis for hydrogenation of nitrobenzene. J Phys Chem B. 1999; 103: 9673-9682.

42. Ichikawa M, Rao L, Ito T, Fukuoka A. Ensemble and ligand effects in selective alkane hydrogenolysis catalyzed on well characterized rhodium-iridium and rhodium-iron bimetallic clusters inside NaY zeolite. Faraday Discuss Chem Soc Rev. 1989; 87: 321-336.

43. Nishiyama S, Kubota T, Kimura K, Tsuruya S, Masai M. Unique hydrogenation activity of supported tin catalyst: Selective hydrogenation catalyst for unsaturated aldehydes. J Mol Catal A-Chem. 1997; 120: L17-22.

44. Murahashi S, Naota T, Hirai N. Aerobic oxidation of alcohols with ruthenium-cobalt bimetallic catalyst in the presence of aldehydes. J Org Chem. 1993; 58: 7318-7319.

45. Dhakad M, Fino D, Rayalu S, Kumar R, Watanabe A, et al. Zirconia supported Ru-Co bimetallic catalysts for diesel soot oxidation. Top Catal. 2007; 42-43: 273-276.

46. Hermans S, Raja R, Thomas JM, Johnson BFG, Sankar G, et al. Solvent-free, low-temperature, selective hydrogenation of polyenes using a bimetallic nanoparticle Ru-Sn catalyst. Angew Chem, Int Ed. 2001; 40: 1211-1215.

47. Ruppert AM, Weinberg K, Palkovits R. Hydrogenolysis goes bio: From carbohydrates and sugar alcohols to platform chemicals. Angew Chem, Int Ed. 2012; 51: 2564-2601.

48. Sankar M, Dimitratos N, Miedziak PJ, Wells PP, Kiely CJ, et al. Designing bimetallic catalysts for a green and sustainable future. Chem Soc Rev. 2012; 41: 8099-8139.

49. Ferrando R, Jellinek J, Johnston RL. Nanoalloys: From theory to applications of alloy clusters and nanoparticles. Chem Rev. 2008; 108: 845-910.

50. Bracey CL, Ellis PR, Hutchings GJ. Application of copper-gold alloys in catalysis: Current status and future perspectives. Chem Soc Rev. 2009; 38: 2231-2243.

51. Toshima N, Yonezawa T. Bimetallic nanoparticles-Novel materials for chemical and physical applications. New J Chem. 1998; 22: 1179-1201.

52. Bönnemann H, Richards RM. Nanoscopic metal particles-Synthetic methods and potential applications. Eur J Inorg Chem. 2001: 2455-2480.

53. Muñoz-Flores BM, Kharisov BI, Jiménez-Pérez VM, Elizondo Martínez P, López ST. Recent advances in the synthesis and main applications of metallic nanoalloys. Ind Eng Chem Res. 2011; 50: 7705-7721.

54. Yu W, Porosoff MD, Chen JG. Review of Pt-based bimetallic catalysis: From model surfaces to supported catalysts. Chem Rev. 2012; 112: 5780-817.

55. Boutonnet M, Sánchez-Domínguez M. Microemulsion droplets to catalytically active nanoparticles. How the application of colloidal tools in catalysis aims to well design and efficient catalysts. Catal Today. 2017; 285: 89-103.

56. Hwang BJ, Sarma LS, Chen JM, Chen CH, Shih SC, et al. Structural Models and Atomic Distribution of Bimetallic Nanoparticles as Investigated by X-ray Absorption Spectroscopy. J Am Chem Soc. 2005; 127: 11140-1145.

57. Somorjai GA, Park JY. Molecular factors of catalytic selectivity. Angew Chem, Int Ed. 2008; 47: 9212 -9228.

58. Liao H, Fisher A, Xu ZJ. Surface segregation in bimetallic nanoparticles: A critical issue in electrocatalyst engineering. Small. 2015; 11: 3221-3246.

59. Boutonnet M, Lögdberg S, Svensson EE. Recent developments in the aplication of nanoparticles prepared from w/o microemulsions in heterogeneous catalysis. Curr Opin Colloid Interface Sci. 2008; 13: 270-286.

60. Eriksson S, Nylen U, Rojas S, Boutonnet M. Preparation of catalysts from microemulsions and their applications in heterogeneous catalysis. Appl Catal A. 2004; 265: 207-219.

61. Fletcher PDI, Howe AM, Robinson BH. The kinetics of solubilisate exchange between water droplets of a water–in-oil microemulsion. J Chem Soc, Faraday Trans. 1987; 83: 985-1006.

62. Tojo C, Blanco MC, López-Quintela MA. Preparation of nanoparticles in microemulsions: A Monte Carlo study of the influence of the synthesis variables. Langmuir. 1997; 13: 4527-4234.

63. Magno LM, Sigle W, Aken PAv, Angelescu DG, Stubenrauch C. Microemulsions as reaction media for the synthesis of bimetallic nanoparticles: Size and composition of particles. Chem Mater. 2010; 22: 6263-6271.

64. Tojo C, de Dios M, López-Quintela MA. On the structure of bimetallic nanoparticles synthesized in microemulsions. J Phys Chem C. 2009; 113: 19145 -1954.

65. Buceta D, Tojo C, Vukmirovik M, Deepak FL, López-Quintela MA. Controlling bimetallic nanostructures by the microemulsion method with sub-nanometer resolution using a prediction model. Langmuir. 2015; 31: 7435-7439.

66. Tojo C, Buceta D, López-Quintela MA. Bimetallic nanoparticles synthesized in microemulsions: A computer simulation study on relationship between kinetics and metal segregation. J Colloid Interface Sci. 2018; 510: 152-1561.

67. Quintillán S, Tojo C, Blanco MC, López-Quintela MA. Effects of the intermicellar exchange on the size control of nanoparticles synthsized in microemulsions. Langmuir. 2001; 17: 7251-7254.

68. Ström L, Ström H, Carlsson P, Skoglundh M, Härelind H. Catalytically active Pd-Ag Alloy nanoparticles synthesized in microemulsion template. Langmuir. 2018; 34: 9754-9761.

69. Guobin W, Wei D, Qian L, Weiliang C, Jingchang Z. Reverse microemulsion synthesis and characterization of Pd-Ag bimetallic alloy catalysts supported on Al_2O_3 for acetylene hydrogenation. China Pet Process Pe 2012; 14: 59-67.

70. Tojo C, Buceta D, López-Quintela MA. On metal segregation of bimetallic nanocatalysts prepared by a one-pot method in microemulsions. Catalysts. 2017; 7: 68-85.